

1

Electronic Supporting Information

2 **Effects of Molecular-Weight-Fractionated Natural Organic Matter on the**

3 **Phytoavailability of Silver Nanoparticles**

4 Min Li,^{ab} Fei Dang,^{*a} Qing-Long Fu,^c Dong-Mei Zhou^a and Bin Yin^d

5 ^a Key Laboratory of Soil Environment and Pollution Remediation, Institute of Soil Science, the

6 Chinese Academy of Sciences, Nanjing 210008, China

7 ^b University of Chinese Academy of Sciences, Beijing 100049, China

8 ^c Department of Civil and Environmental Engineering, Tokyo Institute of Technology, Tokyo 152-

9 8552, Japan

10 ^d State Key Laboratory of Soil and Sustainable Agriculture, Institute of Soil Science, the Chinese

11 Academy of Sciences, Nanjing 210008, China

12

13

14

15

16 ^{*} Corresponding author, Tel: +86-25-86881179, Fax: +86-25-86881000.

17 E-mail: fdang@issas.ac.cn.

18

19 **Summary**

20 **11 SI pages containing 2 tables and 7 figures.**

22 **Contents**

23	Detailed information of NOM (Table S1).....	page S3
24	The washing efficiencies of two washing methods (Table S2).....	page S4
25	The linear pattern of total Ag uptake by rice over time (Figure S1).....	page S5
26	AgNP characterizations (Figure S2).....	page S6
27	TEM images and size distribution of AgNPs incubated with NOM (Figure S3)	page S7
28	Hydrodynamic diameters of NOM alone in the exposure medium (Figure S4)	page S8
29	Correlation between uptake rates and compositional differences (Figure S5)	page S9
30	The chemical structural formulas of the small-NOM models (Figure S6).....	page S10
31	The effects of the NOM concentration, the NOM fractionation, and the small-NOM models on	
32	pH (Figure S7)	page S11

34 **Table S1** Elemental composition and acidic functional groups of Suwannee River natural organic
35 matter (NOM) as provided by the International Humic Substance Society (available at
36 <http://humic-substances.org/#products>).

Sample	H ₂ O	Ash ^a	C	H	O	N	S	P	Carboxyl ^b	Phenolic ^c
NOM	5.69	4.01	50.7	3.97	41.48	1.27	1.78	ND	11.21	2.47

37 ^a: Percentage of inorganic residue (% w/w) in a dry sample.

38 ^b: Charge density (m_{eq} g⁻¹ C) at pH 8.0.

39 ^c: Two times the change in the charge density (m_{eq} g⁻¹ C) between pH 8.0 and pH 10.0.

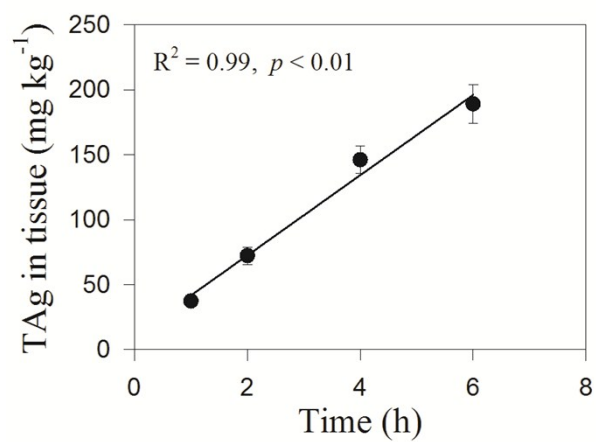
40 ND: not determined.

41

43 **Table S2** Washing efficiencies of two washing methods (HNO₃ + L-cysteine and CaCl₂). HNO₃ +
 44 L-cysteine: tissues were soaked thoroughly in Milli-Q water for 10 min, rinsed with 10 mM HNO₃,
 45 soaked thoroughly in 10 mM of freshly prepared L-cysteine for 20 min, and finally rinsed with
 46 Milli-Q water after soaking in AgNP medium for 2 or 10 min. CaCl₂: tissues were soaked
 47 thoroughly in Milli-Q water for 10 min, 10 mM CaCl₂ for 20 min, and finally rinsed with Milli-Q
 48 water after soaking in AgNP medium for 2 or 10 min. Exposure medium condition: 10 mg AgNPs
 49 L⁻¹ in 1/4 Hoagland's medium (pH 5.6 ± 0.1). The data are presented as the mean ± SD (n = 5).

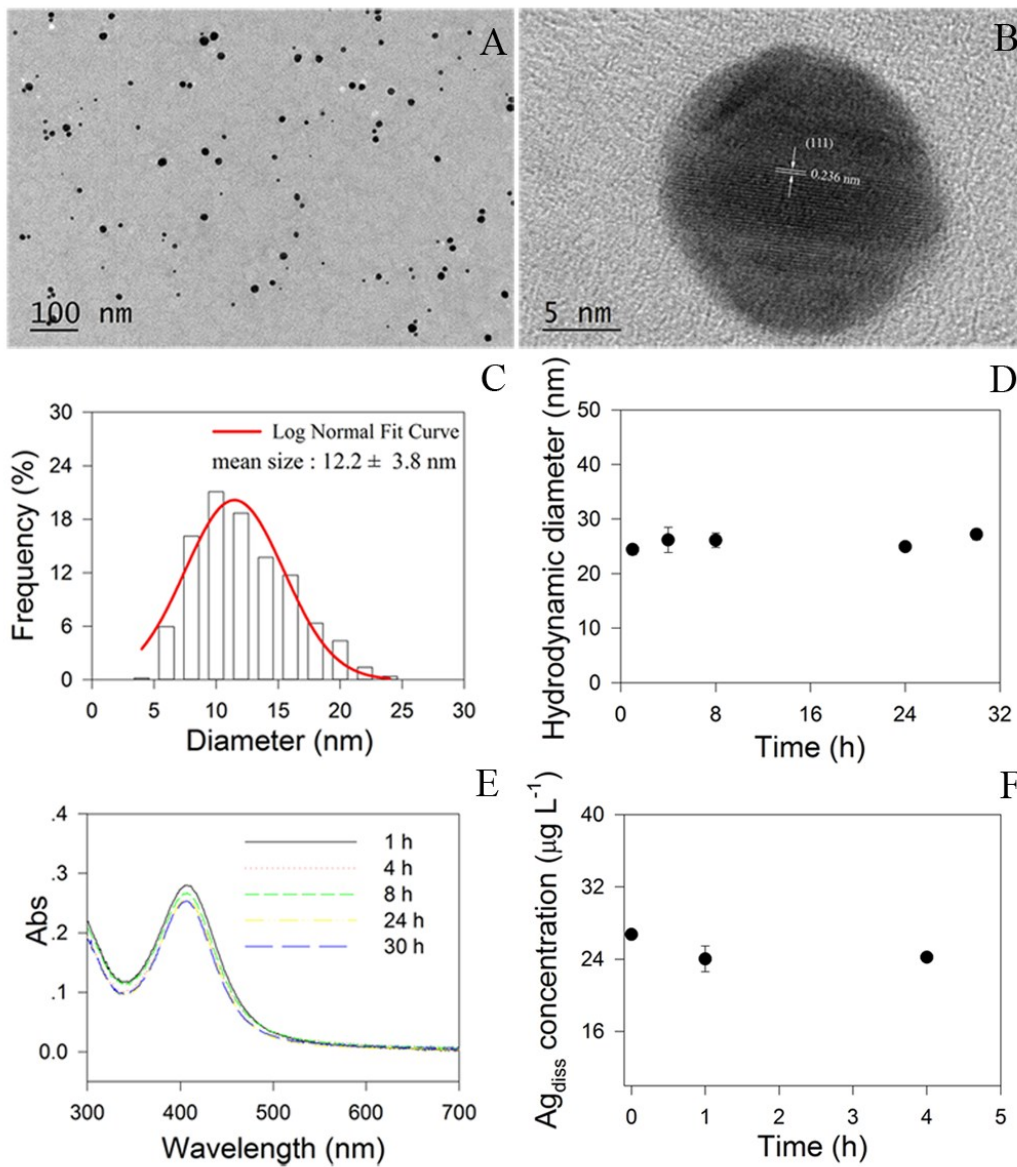
	CaCl ₂ (2 min)	HNO ₃ + L-cysteine (2 min)	CaCl ₂ (10 min)	HNO ₃ + L-cysteine (10 min)
Ag in washing solution (µg)	9.32 ± 1.30	12.40 ± 1.89	12.20 ± 2.05	13.88 ± 2.27
Ag remained in tissue (µg)	3.66 ± 0.82	2.90 ± 0.90	4.31 ± 0.95	2.93 ± 0.66
Ag removed (%)	72.0 ± 2.00	81.4 ± 2.80	74.1 ± 2.08	82.6 ± 2.22

50



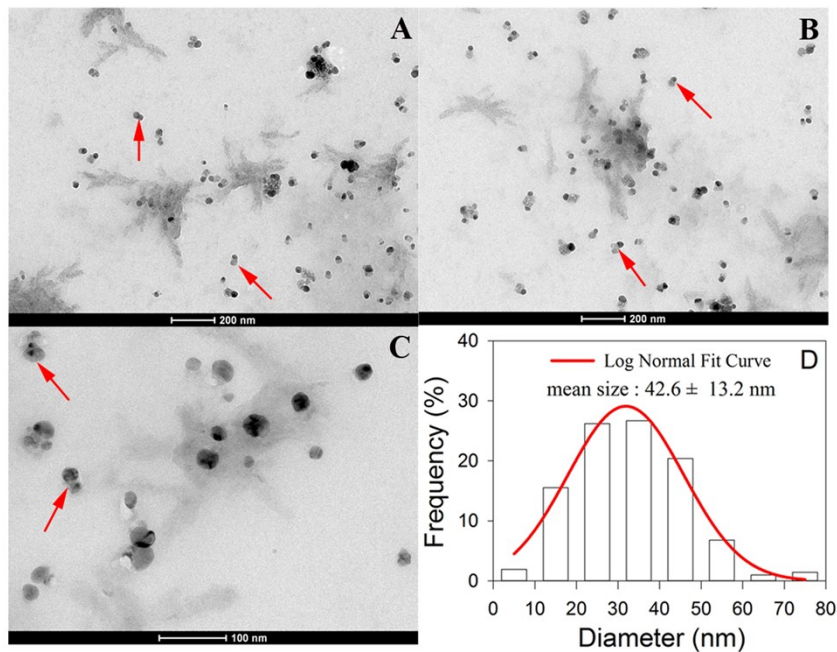
53

54 **Figure S1.** Linear pattern of the uptake of total Ag by rice over time. The data are presented as the
55 mean \pm SD (n = 5). Exposure medium condition: 1 mg AgNPs L⁻¹ in 1/4 Hoagland's medium (pH
56 5.6 \pm 0.1).



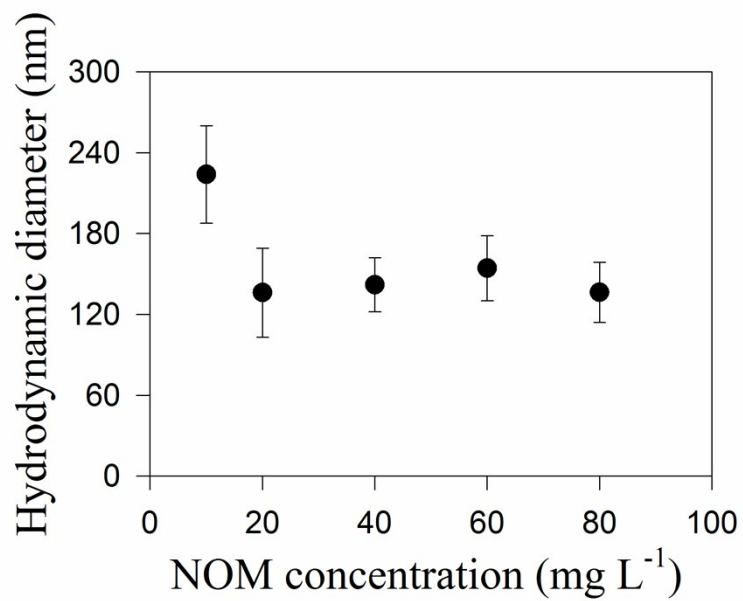
58

59 **Figure S2.** Representative transmission electron microscopy (TEM) image (A), high-resolution
 60 TEM image (B), particle size distribution (C), number-weighted hydrodynamic diameters (D),
 61 UV-Vis spectra (E), and dissolved Ag (Ag_{diss}) concentration (F) of $1 \text{ mg AgNPs L}^{-1}$ in 1/4
 62 Hoagland's medium ($\text{pH } 5.6 \pm 0.1$).



64

65 **Figure S3.** Representative TEM images (A, B, and C) and particle size distribution (D) of AgNPs
 66 incubated with 80 mg L⁻¹ NOM. The AgNP concentration (5 mg L⁻¹) was higher than that in the
 67 exposure medium to satisfy the detection limit of TEM. Note that particle size distribution were
 68 analyzed by 200 well-dispersed nanoparticles with NOM adsorption (as indicated in the selected
 69 particles), while particles associated with large NOM aggregates were not considered.

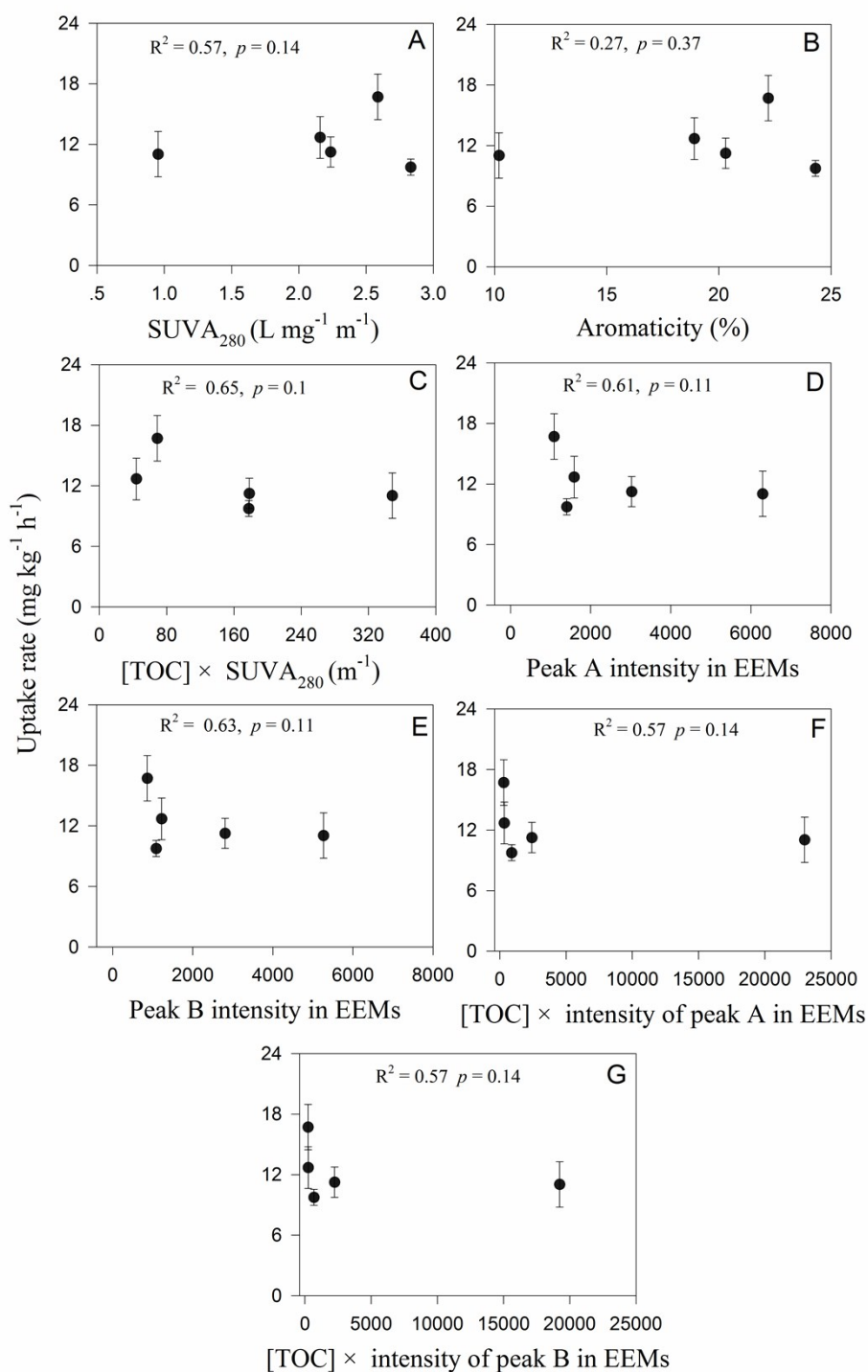


72

73 **Figure S4.** Number-weighted hydrodynamic diameters of NOM alone in the exposure medium:

74 1/4 Hoagland solution at pH 5.6. Samples were prepared using unfractionated NOM ranging from

75 10 to 80 mg L⁻¹. The data are presented as the mean ± SD (n = 5).



77

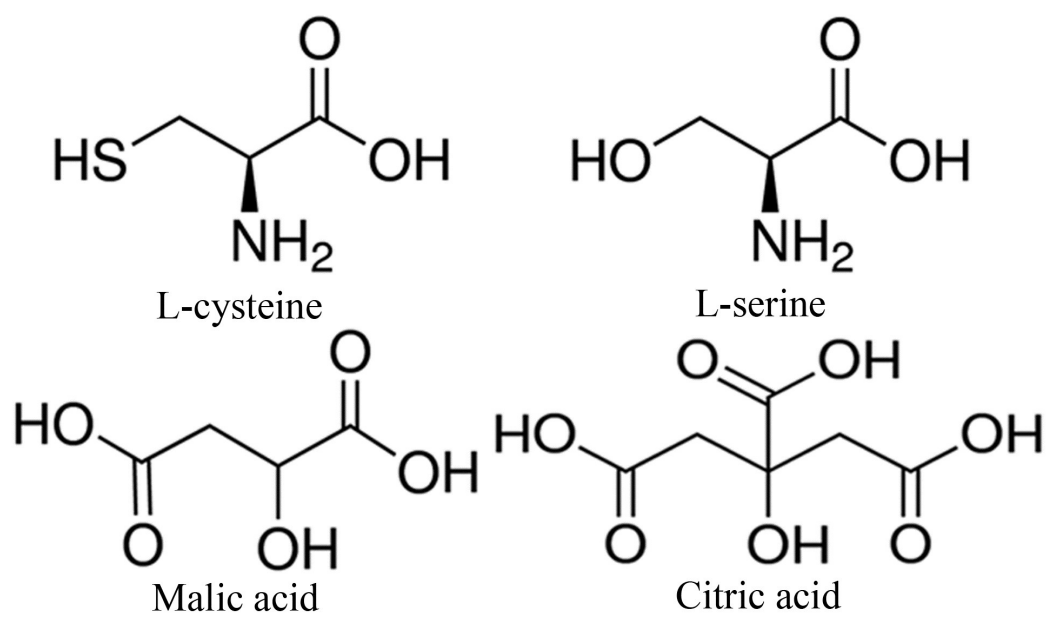
78 **Figure S5.** Correlation between total Ag uptake and the compositional differences in the NOM

79 fractions. A: specific ultraviolet absorbance at 280 nm (SUVA₂₈₀), B: aromaticity, C: [TOC] ×

80 SUVA₂₈₀, D: peak A intensity in the excitation-emission matrix spectra (EEMs), E: peak B

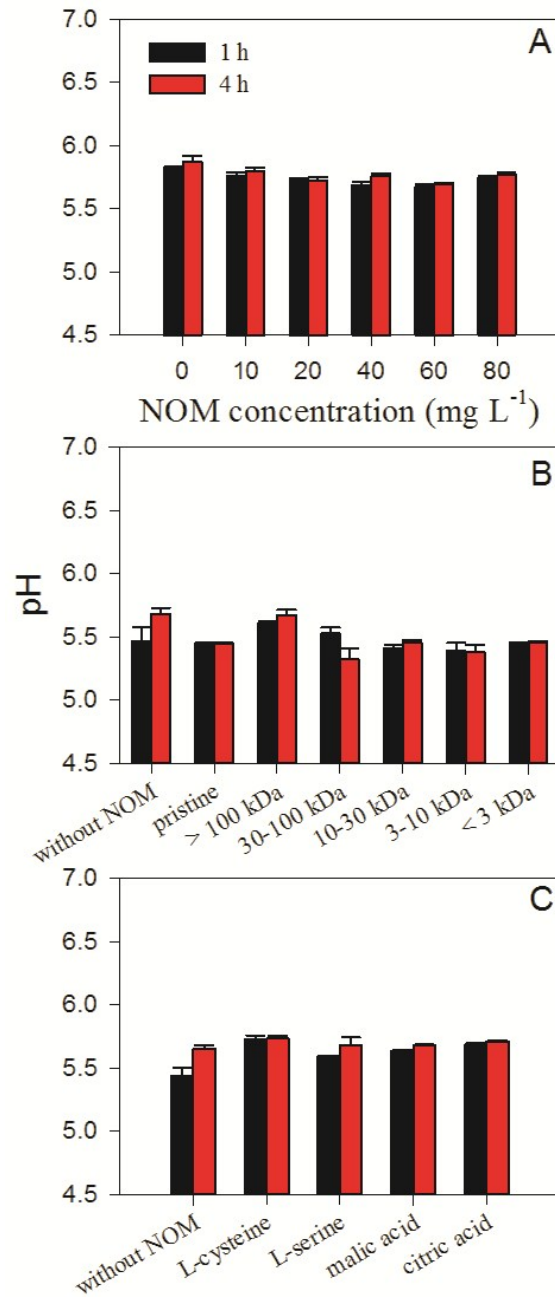
81 intensity in the EEMs, F: [TOC] × intensity of peak A in EEMs, G: [TOC] × intensity of peak B in

82 EEMs.



83

84 **Figure S6.** Chemical structural formulas of small-NOM models.



86

87 **Figure S7.** Effects of NOM concentration (A), NOM fractionation (B), and small-NOM models

88 (C) on the pH of the exposure medium. Exposure medium condition: 1 mg AgNPs L⁻¹ in 1/4

89 Hoagland's medium (pH 5.6 ± 0.1). The data are presented as the mean ± SD (n = 5).